

Patterned distribution of silicon nanocrystals prepared by pulsed laser interference  
crystallization of an ultrathin a-Si:H single layer

This article has been downloaded from IOPscience. Please scroll down to see the full text article.

2003 J. Phys.: Condens. Matter 15 609

(<http://iopscience.iop.org/0953-8984/15/4/301>)

View [the table of contents for this issue](#), or go to the [journal homepage](#) for more

Download details:

IP Address: 171.66.16.119

The article was downloaded on 19/05/2010 at 06:30

Please note that [terms and conditions apply](#).

# Patterned distribution of silicon nanocrystals prepared by pulsed laser interference crystallization of an ultrathin a-Si:H single layer

Xiaowei Wang<sup>1</sup>, Feng Qiao<sup>1</sup>, Leyi Zhu<sup>1</sup>, Xinfan Huang<sup>1,3</sup>, Jian Li<sup>1</sup>, Wei Li<sup>1</sup>, Xuefei Li<sup>1</sup>, Lin Kang<sup>2</sup> and Kunji Chen<sup>1</sup>

<sup>1</sup> National Laboratory of Solid State Microstructures and Department of Physics, Nanjing University, Nanjing 210093, People's Republic of China

<sup>2</sup> Department of Electronic Science and Engineering, Nanjing University, Nanjing 210093, People's Republic of China

Received 17 July 2002, in final form 11 November 2002

Published 20 January 2003

Online at [stacks.iop.org/JPhysCM/15/609](http://stacks.iop.org/JPhysCM/15/609)

## Abstract

We employ the method of phase-modulated KrF excimer pulsed laser interference crystallization (LIC) to fabricate nanocrystalline silicon with a two-dimensional (2D) patterned distribution within an ultrathin a-Si:H single layer. A local phase transition occurs in the ultrathin a-Si:H film upon LIC with the appropriate energy density. The results from atomic force microscopy, Raman scattering spectroscopy, planar and cross-sectional transmission electron microscopy and scanning electron microscopy demonstrate that Si nanocrystallites are formed within the initial a-Si:H single layer, selectively located in disc-shaped regions with diameters of 250 nm and patterned with the same 2D periodicity of 2.0  $\mu\text{m}$  as the phase-shifting grating.

(Some figures in this article are in colour only in the electronic version)

## 1. Introduction

Nanocrystalline silicon (nc-Si) has long been a focus of great interest due to its potential application in future optoelectronics and nano-electronics [1–7]. For the purpose of device application, in general, patterned nc-Si structures are necessary [8]. However, for patterned generation, the standard technique of optical lithography is limited by its poor resolution capability and its indirectness. Although the focused electron beam or ion beam technique overcomes the shortcomings of optical lithography, it requires expensive equipment and its yield is low for large-scale production due to its serial scanning process. Therefore, it is also limited as regards wide use.

<sup>3</sup> Author to whom any correspondence should be addressed.

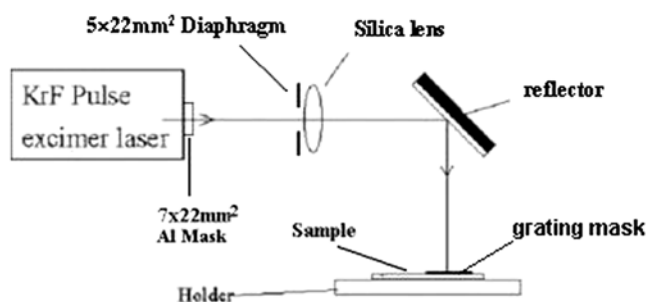


**Figure 1.** The schematic experimental set-up for laser-induced crystallization.

In the last decade, the method of pulsed laser interference crystallization (LIC) with a two-beam/multi-beam interference system has been reported, for preparing microcrystalline silicon ( $\mu\text{c-Si}$ ) films. By this method, a one-dimensional/two-dimensional interference pattern is achieved [9–11]. In our previous work, by the method of phase-modulated KrF excimer pulsed LIC, we have successfully fabricated one-dimensional (1D) self-organized Si dots in a-Si:H films which are 50 nm thick [12]. Further, by means of LIC we realized constrained crystallization [13, 14] of ultrathin a-Si:H sublayers within a-Si:H/a-SiN<sub>x</sub>:H multilayers and controlled the transverse and longitudinal positions of nc-Si dots to achieve three-dimensional ordered distribution of nc-Si [13, 14].

In this paper, we attempt to realize two-dimensional (2D) ordered distribution of nc-Si in the plane of an ultrathin a-Si:H single layer. The phase-modulated LIC method is again employed to crystallize ultrathin a-Si:H film with the thickness of only 10 nm. Simply by combining a 2D phase-shifting grating with our pulsed laser irradiation system, a periodic high-intensity-contrast patterned energy distribution is achieved on the surface of a-Si:H film [15]. Upon pulsed laser irradiation, a new kind of nc-Si material has been fabricated over large areas, where nc-Si dots were locally formed in ultrathin a-Si films in the form of regularly patterned 2D arrays. Under optimized conditions, the patterned arrays are composed of nc-Si dots with uniform sizes.

## 2. Experimental details

Ultrathin a-Si:H single-layer films were prepared by decomposition of silane (SiH<sub>4</sub>) on SiO<sub>2</sub>/Si substrate using plasma-enhanced chemical vapour deposition (PECVD) with the following typical parameters: rf power 30 W, substrate temperature 250 °C, reaction pressure 16 Pa, deposition rate about 0.1 nm s<sup>-1</sup>. The thickness of the a-Si:H films was 10 nm. SiO<sub>2</sub>/Si substrates were prepared by means of thermal oxidization of (100) Si wafer; the SiO<sub>2</sub> layer was about 500 nm thick.

The crystallization of a-Si:H thin films was performed by laser irradiation with a pulsed (30 ns) KrF ( $\lambda = 248$  nm) excimer laser at room temperature. The laser beam is focused, by a fused quartz lens ( $f = 24$  cm), to increase its energy density. The exposure areas in the surfaces of thin films can be varied from  $5 \times 20$  to  $5 \times 4$  mm<sup>2</sup> in our experimental system. During the LIC treatment, a sample was placed just below the phase-shifting grating mask. The surface-relief 1D and 2D phase-shifting gratings, which were used in the laser-patterned local crystallization experiment, are designed with 2  $\mu\text{m}$  periodicity and 260 nm depth. Upon laser irradiation, a transient thermal 1D grid and 2D matrix are directly formed on the surface of the sample, leading to the local crystallization of the a-Si:H films. Figure 1 shows the experimental set-up.

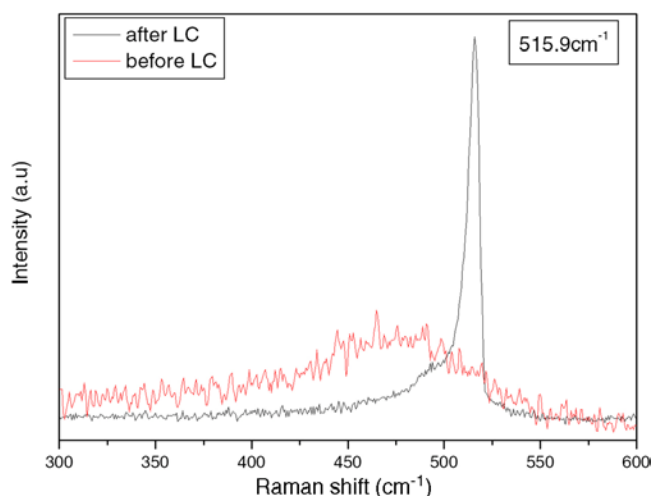


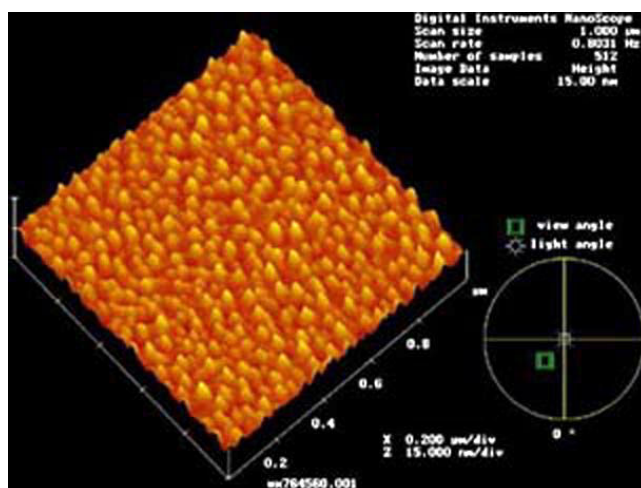
**Figure 2.** The Raman scattering spectra of the sample before and after laser crystallization without the phase-shifting grating mask. There is a broad peak at around  $480\text{ cm}^{-1}$  and a sharp peak at  $515.9\text{ cm}^{-1}$ .

The crystallinity, morphology and microstructures of crystallized samples are then characterized by atomic force microscopy (AFM), Raman scattering spectroscopy, planar and cross-sectional transmission electron microscopy (TEM) and scanning electron microscopy (SEM). The Raman measurements are made on a T64000 Raman system with excitation by the  $514.5\text{ nm}$  wavelength of an  $\text{Ar}^+$  laser in back-scattering geometry with about  $1\text{ mm}$  measurement area. The TEM measurements are performed with JEM200CX microscope working at  $200\text{ kV}$ . The AFM equipped with a Nanoscope III system (Digital Instruments, USA) is employed in contact mode. The SEM analysis is carried on a LEO-1550 SEM system.

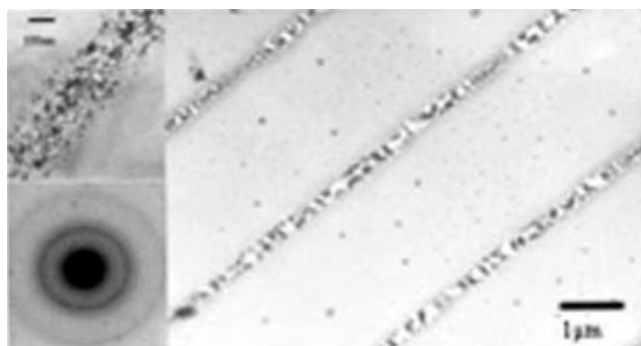
### 3. Results

Figure 2 shows the Raman scattering spectra of the sample after laser-induced crystallization without the phase-shifting grating mask. The energy density of the laser is  $162\text{ mJ cm}^{-2}$  for a single shot. A sharp peak around  $515.9\text{ cm}^{-1}$  corresponding to the TO mode of nc-Si, with a weak shoulder corresponding to the TO mode of a-Si, demonstrates that nc-Si has formed in the sample. The average grain size for the nc-Si is estimated to be  $4.7\text{ nm}$  according to the phonon confinement model [16]. Meanwhile, we calculate the fractions of nc-Si in the sample, defining the crystallinity fraction ratio  $[I_c]/([I_c]+[I_a])$  where  $I_c$  and  $I_a$  are the integrated areas of the TO peaks of nc-Si and a-Si respectively. The fraction of crystalline Si is about 85%. This means that almost all the a-Si in the as-deposited layer is transformed to nanocrystallites.

The AFM results for the sample shown in figure 2 are shown in figure 3. It is clear that the sample is composed of densely packed Si grains with lateral sizes of about  $20\text{ nm}$  and longitudinal sizes of about  $10\text{ nm}$ . We calculate the density of the nc-Si grains by counting the grains in an area of  $5\text{ }\mu\text{m} \times 5\text{ }\mu\text{m}$ . The result shows that the density is about  $4 \times 10^{10}\text{ cm}^{-2}$ . Comparing with the results from Raman spectra, the size of the nc-Si grains obtained from the AFM image is larger. We consider that this is due to every Si grain possibly being made up of several crystalloids with smaller sizes.



**Figure 3.** An AFM photograph of the morphology of the sample shown in figure 2.



**Figure 4.** The planar TEM photograph of the sample after laser irradiation with energy density  $50 \text{ mJ cm}^{-2}$  in front of the 1D grating. One inset shows a magnified view of one stripe. Another inset shows an ED pattern for the Si stripes.

On the basis of the above results, we attempt to control the lateral positions in the nc-Si in the  $x$ -direction by employing the 1D phase-shifting grating first. Figure 4 is a planar TEM photograph of the sample after laser irradiation (with energy density  $50 \text{ mJ cm}^{-2}$  in front of the 1D grating). Stripe-like dark (200 nm) and white areas are alternately arranged with a periodicity of  $2 \mu\text{m}$ , the same as that of the grating. Only in the dark areas can a solid-phase crystallization take place where the energy density exceeds the crystallization threshold [17]. According to theoretical calculations, the energy of the laser in the dark region is four times the original energy in front of the 1D grating, so in the dark region the intensity is about  $200 \text{ mJ cm}^{-2}$ . We can observe that the density of the nanocrystallites ( $2 \times 10^{11} \text{ cm}^{-2}$ ) in the dark region after LIC is higher than the previous density obtained without the grating mask. The magnified part of the stripe shown in the inset of figure 4 indicates that the interfaces between the crystallized and the amorphous zones are abrupt due to the well-defined intensity threshold for laser crystallization of a-Si film. Another inset of figure 4 gives an electron diffraction (ED) pattern for the nc-Si stripe, which indicates that Si crystallites have been formed and embedded in the a-Si matrix. The preferred orientations of these Si crystallites are (111) and (311).

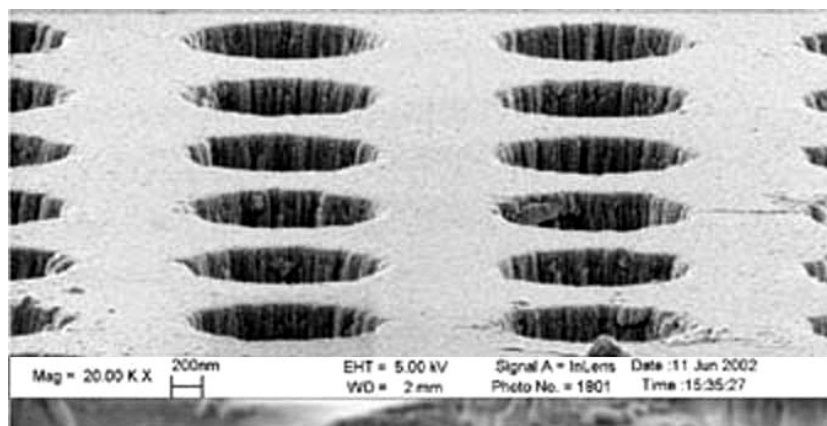


**Figure 5.** An SEM photograph of the surface-relief structure of the 2D phase-shifting grating.

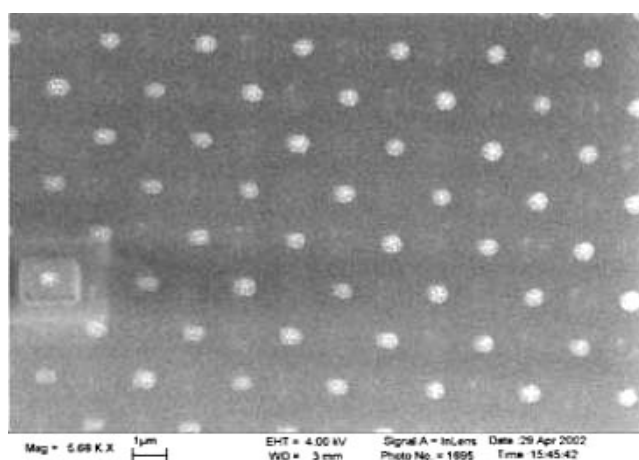


**Figure 6.** An SEM photograph (top view) of a similarly structured sample after LIC with an energy density of  $30 \text{ mJ cm}^{-2}$  in front of the 2D grating.

Further, we use the 2D phase-shifting grating to fabricate a 2D patterned distribution of nc-Si in the  $x$ - and  $y$ -directions. Figure 5 is an SEM photograph of the surface-relief structure of the 2D phase-shifting grating mask. We can see that its periodicity is  $2 \mu\text{m}$ , as designed. Figure 6 shows an SEM image of the sample after LIC with the 2D grating mask, whose energy density is  $30 \text{ mJ cm}^{-2}$  in front of the 2D grating. A 2D submicrometre pattern (formed by crystallized zones in a-Si:H films) is clearly revealed. The white discs (crystallized zones) with diameter  $250 \text{ nm}$  and period  $2 \mu\text{m}$  are each composed of several Si crystallites. The grey regions around the white discs correspond to the remaining amorphous Si, the flat surface of which is retained after irradiation. Moreover, the morphologies of all discs are nearly the same, which demonstrates that the LIC method is effective for fabricating nc-Si patterns. In addition, the crystallized zones on the surface gradually disappeared with the decrease of the laser energy density. The surface of the sample irradiated with the energy density of  $25 \text{ mJ cm}^{-2}$  is almost smooth and so no periodic discs on the surface of this sample were observed in AFM measurements. By the cross-sectional TEM technique, we successfully

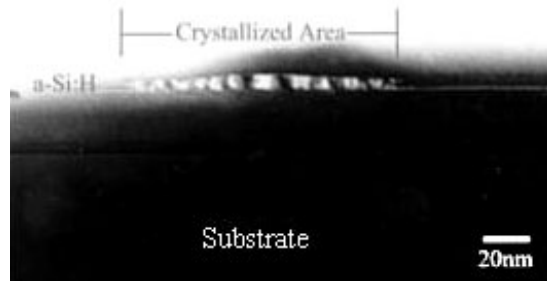


**Figure 7.** A cross-sectional TEM photograph of crystallization regions in the ultrathin a-Si single layer after LIC.

observed the microstructure of the crystallization regions shown in figure 7; this confirms the formation of Si crystallites in the as-deposited ultrathin a-Si layer after LIC. It clearly shows that the Si crystallites are closely arranged one by one in the crystallized area. The size of the crystallites in the middle of the regions is larger than that of the crystallites on the border because of the higher laser energy. The interface between the crystallized and the amorphous zones is also abrupt after laser irradiation.

We compare our LIC method with the thermal crystallization method. To produce nc-Si through thermal crystallization, high-temperature treatment is necessary, which is undesirable in device processing. On the other hand, the thermal annealing technique cannot produce patterned crystallization. In contrast, our method is a low-temperature process and can produce patterned crystallization, which is of particular importance since patterned nc-Si structures are required for device fabrications.

#### 4. Conclusions

In summary, we utilized AFM, Raman scattering spectroscopy, TEM and SEM to investigate the surface morphology and the structural properties of an ultrathin a-Si:H single layer deposited on a SiO<sub>2</sub>/Si substrate, which was fabricated by PECVD and then crystallized by laser irradiation. The experimental results show that nc-Si is formed in certain regions with the same periodicity of 2.0  $\mu\text{m}$  as the phase-shifting grating mask. In particular, the patterned distribution of nc-Si can be varied by changing the geometry of the phase-shifting grating mask, using the 1D grating for getting a 1D ordered distribution of nc-Si and the 2D grating for getting a 2D distribution. The surface morphology of the samples can be controlled by means of the laser energy density. So the method of pulsed LIC is one of the most promising methods for fabricating patterned nc-Si at low temperature and is compatible with standard microelectronic processing.

#### Acknowledgments

We would like to give special thanks to Professor Jun Xu of NJU for useful discussions and Professor Xiaoning Zhao and Jiancang Shen of NJU for TEM and Raman measurements. The authors would also like to acknowledge the support of the State Key Programme for Basic Research of China (Grant No 2001 CB 610503), the National Nature Science Foundation of China (Grant Nos 90101020 and 60071019) and the Natural Science Foundation of Jiangsu Province (BK2001028, BG2001002). This work was also partly supported by the NPTND of Korea MOST.

## References

- [1] Canham L T 1990 *Appl. Phys. Lett.* **57** 1046
- [2] Tsybeskov L, Hirschman K D, Duttagupta S P, Zacharias M, Fauchet P M, McCaffrey J P and Lockwood D J 1998 *Appl. Phys. Lett.* **72** 43
- [3] Gu X, Qin H, Lu H, Chen K and Huang X 1996 *J. Non-Cryst. Solids* **227** 1168
- [4] Chen K J, Huang X F, Xu J and Feng D 1992 *Appl. Phys. Lett.* **61** 2069
- [5] Banin U, Cao Y W, Katz D and Millo O 1999 *Nature* **400** 542
- [6] Yoffe A D 2001 *Adv. Phys.* **50** 1
- [7] Wakayama Y, Tagami T and Tanaka S 1999 *Thin Solid Films* **350** 300
- [8] Striemer C C, Krishnan R and Fauchet P M 2001 *Nano Lett.* **1** 643
- [9] Dahlheimer B, Karrer U, Nebel C E and Stutzmann M 1998 *J. Non-Cryst. Solids* **227–230** 916
- [10] Heintze M, Santos P V, Nebel C E and Stutzmann M 1994 *Appl. Phys. Lett.* **64** 3148
- [11] Nebel C E 1996 *Mater. Res. Soc. Symp. Proc.* **420** 117
- [12] Chen K J *et al* 1998 *J. Non-Cryst. Solids* **227–230** 934
- [13] Huang X F, Li Z F, Liu Z G and Chen K J 1996 *J. Non-Cryst. Solids* **198–200** 821
- [14] Huang X F *et al* 2000 *J. Non-Cryst. Solids* **266–269** 1015
- [15] Jiang M, Wang M X and Chen K J 1999 *Chin. J. Lasers B* **8** 142
- [16] Chen G X, Chen K J and Zhang X K 1992 *Phys. Status Solidi a* **129** 421
- [17] Wang L, Li J, Huang X F, Li W and Chen K J 2000 *Appl. Surf. Sci.* **165** 85